SCIENCE CHINA
Technological Sciences

December 2010 Vol.53 No.12: 3302–3309
doi: 10.1007/s11431-010-4175-1

Performance prediction and flow analysis in the vaned distributor of a pump turbine under low flow rate in pump mode

YIN JunLian[1], LIU JinTao[1], WANG LeQin[1], JIAO Lei[1], WU DaZhuan[1*] & QIN DaQing[2]

[1] *Institute of Chemical Machinery, Department of Chemical and Biological Engineering, Zhejiang University, Hangzhou 310027, China;*
[2] *Harbin Institute of Large Electrical Machinery, Harbin 150001, China*

Received June 18, 2010; accepted October 20, 2010

The main goal of this work is to investigate the possible different flow patterns existing in pump turbine under off-design conditions in pump mode. Numerical simulations by solving the Navier-Stokes equation, coupled with the "SST k-ω" turbulence model, were carried out. Flow characteristics were assumed to be stalled in the appropriate region of flow rate levels of Q/Q_D=0.15–0.61. The simulation result was compared with experimental data and they showed good agreement. Consequently, velocity fields in three axial locations in stay vanes and guide vanes were analysed in details. It was shown that "jet-wake" flow pattern exists near the band, which changes little in the whole shape with flow rate increasing; to the middle location of vanes, reverse flow begins to appear on the interface between the runner and guide vanes, which will disappear gradually as the flow rate increases; massive reverse flow is captured near the crown, whose intensity will be weakened as the flow rate increases. Ultimately, it was found that the special head-flow profile can be ascribed to the special hydraulic loss characteristics of the stay vanes and guide vanes.

pump turbine, flow simulation, stalled flow, guide vane

Citation: Yin J L, Liu J T, Wang L Q, et al. Performance prediction and flow analysis in the vaned distributor of a pump turbine under low flow rate in pump mode. Sci China Tech Sci, 2010, 53: 3302–3309, doi: 10.1007/s11431-010-4175-1

Nomenclature

- b: Spanwise distance (m)
- B: Distance from band to crown (m)
- H: Head (m)
- H_D: Rated Head (m)
- Q: Flow rate ($kg \cdot s^{-1}$)
- Q_D: Rated flow rate ($kg \cdot s^{-1}$)
- $y+$: Dimensionless wall distance
- η: Hydraulic efficiency

1 Introduction

Although there have been many studies on the stalled flow in pumps and compressors, the flow mechanism is still not understood clearly so far. Emmons et al. [1] gave a logical explanation for stalled flow on the basis of cascade theory. Ulrik et al. [2] captured the rotating stall frequency for two different pumps with the help of power spectrum analysis to the experimental data. Krause et al. and Manish et al. carried out flow measurement to centrifugal pumps using the PIV, and interesting flow structures including the "Jet-Wake" flow pattern were found in the vaned diffuser [3, 4]. They also found that the flow in a stalled diffuser passage and the occurrence of stall did not vary significantly with blade orientation. Recently, with the rapid development of computational fluid dynamics (CFD), numerical study for stalled flow is becoming popular. Guleren [5] carried out the simulation to study the stalled flow in a vaned centrifugal pump by using a commercial software, and it was ob-

*Corresponding author (email: wudazhuan@zju.edu.cn)

served that the vane diffuser exerts a significant effect on the pump performance. Tsukamoto [6] proposed an intergration method which coupled the 3D modeling of pump with 1D pipe system to investigate the performance prediction of a diffuser pump under off-design conditions. As to pump turbine, numerical studies mainly have concentrated on the operating conditions near the design point [7, 8], with few relevant numerical simulations on the off-design prediction. Hongjun Ran [9] studied the applicability of different turbulence models for off-design prediction in pump mode and concluded that the S-A model is capable of predicting the hump zone of the head-flow profile. In a word, although the stalled flow was observed in pump turbine, the flow mechanism is not clear so far. Therefore, we aim to investigate the stalled flow patterns by the tools of CFD.

The structure of the article is arranged as follows.Section 2 describes the concerned physical model, in which geometry specifications and operating parameters are listed. Section 3 gives details of numerical setup. Section 4 presents the numerical results, including the velocity vectors at different locations as well as the whole hydraulic losses analysis, followed by the conclusion in Section 5.

2 Description of problem

To consider the non-axisymmetric flow characteristics brought by the flow impingement, the whole configuration including the spiral casing, stay vane and guide vane, runner and draft tube is established as shown in Figure 1. The specific parameters are listed in Table 1. Eight operating points which are bellow Q/Q_D=0.61 are chosen as the simulation objectives.

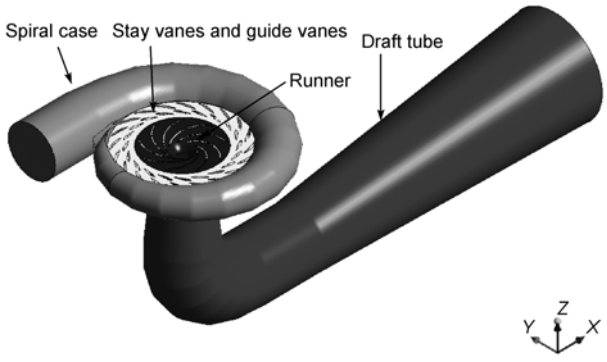

Figure 1 Full three-dimentional pump turbine model.

Table 1 Main characteristics of the tested pump turbine(pump mode)

Runner diameter at inlet (mm)	300
Runner diameter at outlet (mm)	410
Runner blade number	9
Guide vane number	20
Stay vane number	20
Specific speed (N_q)	50

3 Numerical modeling

3.1 Grid generation

The geometry model of the pump turbine was established using the UG commercial software. It has nine backward curved blades, twenty guide vanes and twenty stay vanes. The detailed geometry parameters are listed in Table1 and the whole configuration can be seen in Figure 1.

In the present study, FLUENT has been used for calculation, with transport equations solved by finite volume method. Hybrid mesh was generated to define the flow zone which is subdivided into three parts (spiral casting and vanes, runner, draft tube). The whole mesh was generated on the platform of ICEMCFD and illustrated in Figure 2. Mixed mesh generation method was adopted to make up the computational domain consisting of tetrahedral elements in the spiral casing, guide vanes, stay vanes, and hetrahedral elements in runner and draft tube. Figure 3 is a sketch map of the hybrid grid for stay vanes and guide vanes and an enlarged view of grid for boundary refinement of blade is shown in Figure 4. After computational test, it is proved that the grid system can satisfy the requirement of the SST turbulence model,

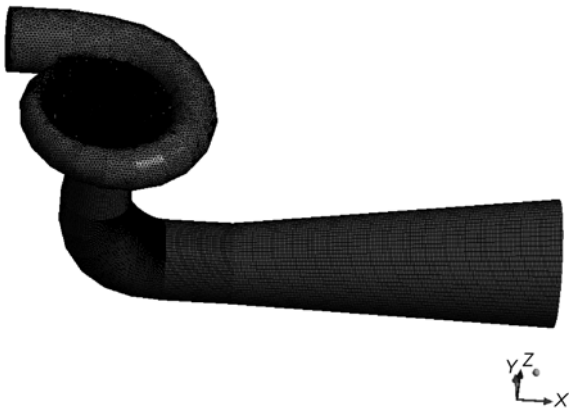

Figure 2 Mesh generation for the whole configuration.

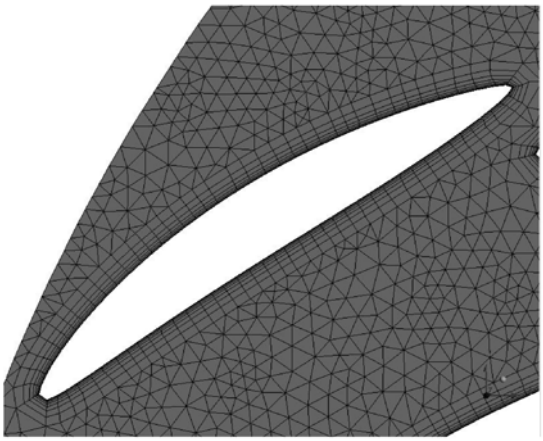

Figure 3 Hybrid mesh for guide vanes and stay vanes.

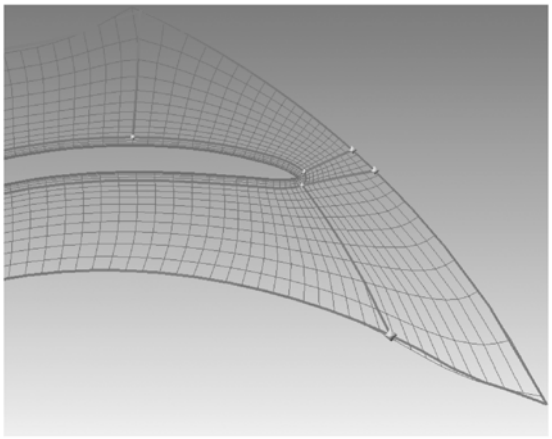

Figure 4 An enlarged picture of the runner grid.

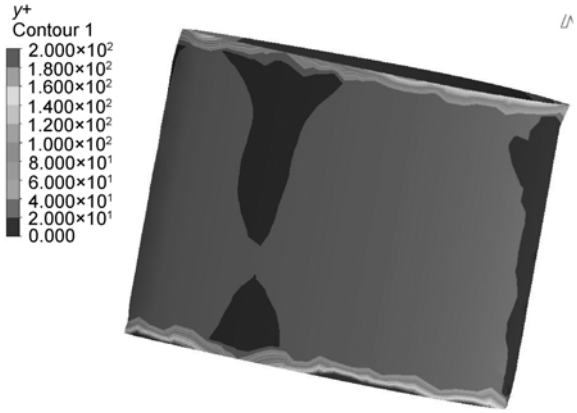

Figure 5 Contour of *y*+ on the wall of guide vane

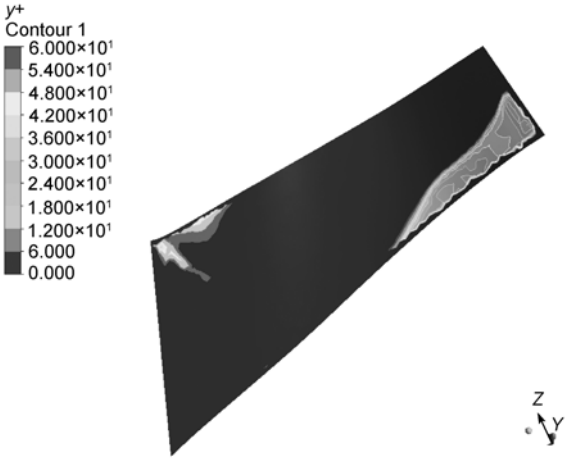

Figure 6 Contour of *y*+ on the wall of runner vane.

which can be seen from the *y*+ values on the walls of guide vanes and runner vanes displayed in Figures 5 and 6, respectively. The details of the grid generation are listed in Table 2. In summary, the total number of cells adds up to 10945549.

3.2 Boundary conditions

3.2.1 Inlet boundary conditions

The velocity inlet at draft tube is used, whose profile is assumed to be uniform and determined by the experiment. The total pressure is specified at the inlet boundary, and thus, the static pressure can be decided in the initialization. The turbulence parameters are specified in terms of turbulence intensity and hydraulic diameter of the inlet.

3.2.2 Outlet boundary conditions

Pressure outlet is used at spiral casing, static pressure (p=0 Pa) is specified for all cases since the aim of the study is focused on the energy characteristics.

3.2.3 Other conditions

No-slip condition is assumed on all the solid walls, and standard wall function is used to calculate the turbulence kinetic energy and turbulence dispassion frequency near the wall. The rotation of runner domain is considered by the use of the multiple rotating reference frame (MRF) method.

3.3 Solution strategy

FLUENT is used to carry out the numerical simulations. The code solves the Reynolds averaged Navier–Stokes equations in a primitive variable form. The effects of turbulence are modeled using the SST k-ω turbulence in the simulation. The second-order upwind scheme is used for discretization of convective term and the second-order central difference scheme for discretization of diffusion term. The separated solver is used to solve the incompressible flow. Numerical convergence is set to a maximum of 1×10^{-4}.

Table 2 Mesh characteristics of the computational domain

Components	Cell number	Mean *y*+	Cell type
Spiral casing	2001264	115	Tetrahedron
Stay vanes, guide vanes	3435236	55	Hybrid
Runner vanes	4002457	60	Hexahedron
Draft tube	1506592	200	Hexahedron

4 Results and discussions

As a reality check, the performance curve is predicted with various flow rates as follows: Q/Q_D=0.07, 0.15, 0.23, 0.28, 0.37, 0.43, 0.47, 0.53 and 0.61. Figures 7 and 8 show the comparisons between computational results and model test data on the basis of the head-flow profile and flow- efficiency profile. To check the accuracy of numerical modeling, a simple error study for the flow-head profile is used. The relative error is less than 3%, indicating that the numerical method is reliable and the results can be used to analyze the flow fields. Due to obvious difference between

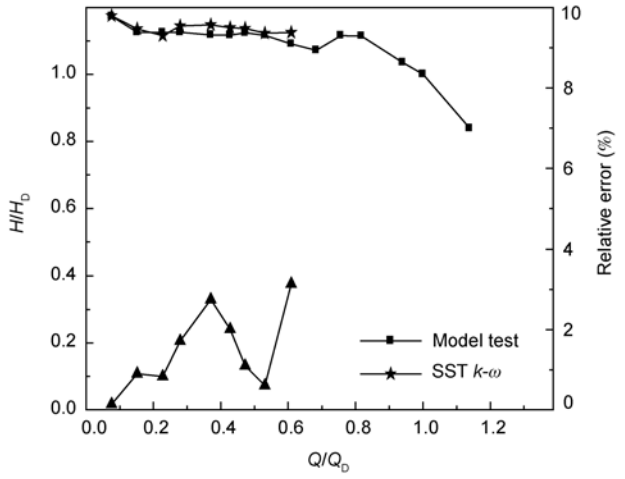

Figure 7 Comparison for head-flow between computational results and experimental data.

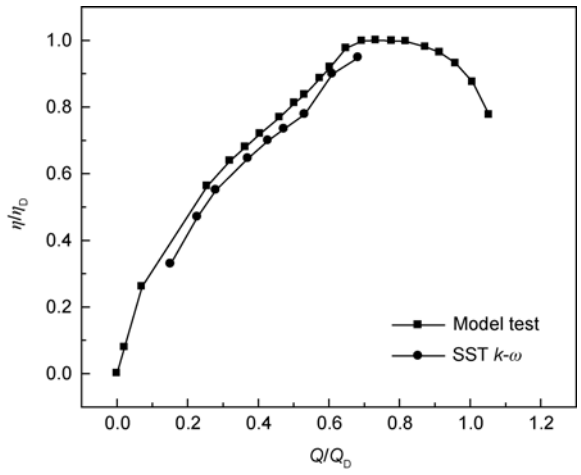

Figure 8 Comparison for efficiency-flow between computational results and model test data.

point Q/Q_D=0.07 and others, it is out of the scope in this study. The other eight operating points were selected. The specific notations used in the flow field analysis are depicted in Figure 9. Three blade-to-blade locations from band to crown (b/B=0.1, 0.5, 0.9) noted by P0.1, P0.5 and P0.9, respectively are used to describe the flow patterns in detail in the following sections.

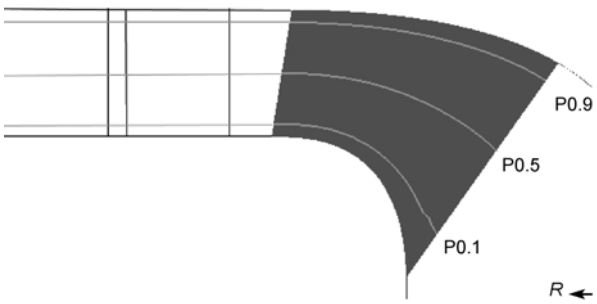

Figure 9 Schematic of cross-sections studied in flow analysis.

4.1 Cross-section I: P0.1

Figure 10 shows the velocity vectors in stay vanes and guide vanes under the eight operating conditions, which can reflect the evolution of the stalled flow clearly. In the whole, obvious the "jet-wake" feature exists under all the operating points, as can be seen from the amplification of part of vanes shown in Figure 11. The main flow structure mainly includes jet flow with high outward radial velocity on the concave side of the guide vanes and stay vanes and wake flow with low or even negative radial velocity on the convex side. The mechanism for its occurence may be ascribed to the large angle of incidence due to flow angle violation. Moreover, flow separation will occur on the convex side of vanes and extend across the whole length of chord of stay vanes and guide vanes. As the flow rate increases, the whole trend for the flow pattern does not change obviously, but its circumference direction in the distribution and the influence of the spiral flow inside have significant changes. In Figure 8(a), the jet intensity is not distributed evenly in the circumference direction, leading to complex vortex structures in the spiral casing. But when Q/Q_D is equal to or greater than 0.23, non-symmetric distribution of "jet-wake" flow can be seen and has more and more effects on the flow in spiral casing in the sense of the jet length, which may be the possible reason for the large radial forces under off-design conditions [9, 10].

4.2 Cross-section II: P0.5

Velocity vectors on P0.5 under the eight operating points are depicted in Figure 12. Large differences can be identified in comparison with P0.1. Firstly, reverse flow is observed in the interface between the runner and guide vanes, suggesting that large adverse pressure gradient is encountered. Secondly, the jet intensity decreases dramatically. With the increase of flow rate, the flow will experience three different phases. When Q/Q_D is less than 0.28, the distribution of velocity in circumferential direction is very irregular in company with backflow. Then this irregularity will be improved as the flow rate increases, as can be seen in Figures 12(d)–(g), in which the "jet-wake" feature will appear. However, when Q/Q_D=0.61, a strange phenomenon appears in that there is no axisymmetry in the domain with several jet flows in a chaotic manner. This transition may have something to do with the hump zone of head-flow profile which is out of the scope of this study.

4.3 Cross-section III: P0.9

Figure 13 presents velocity vectors on P0.9 under all the

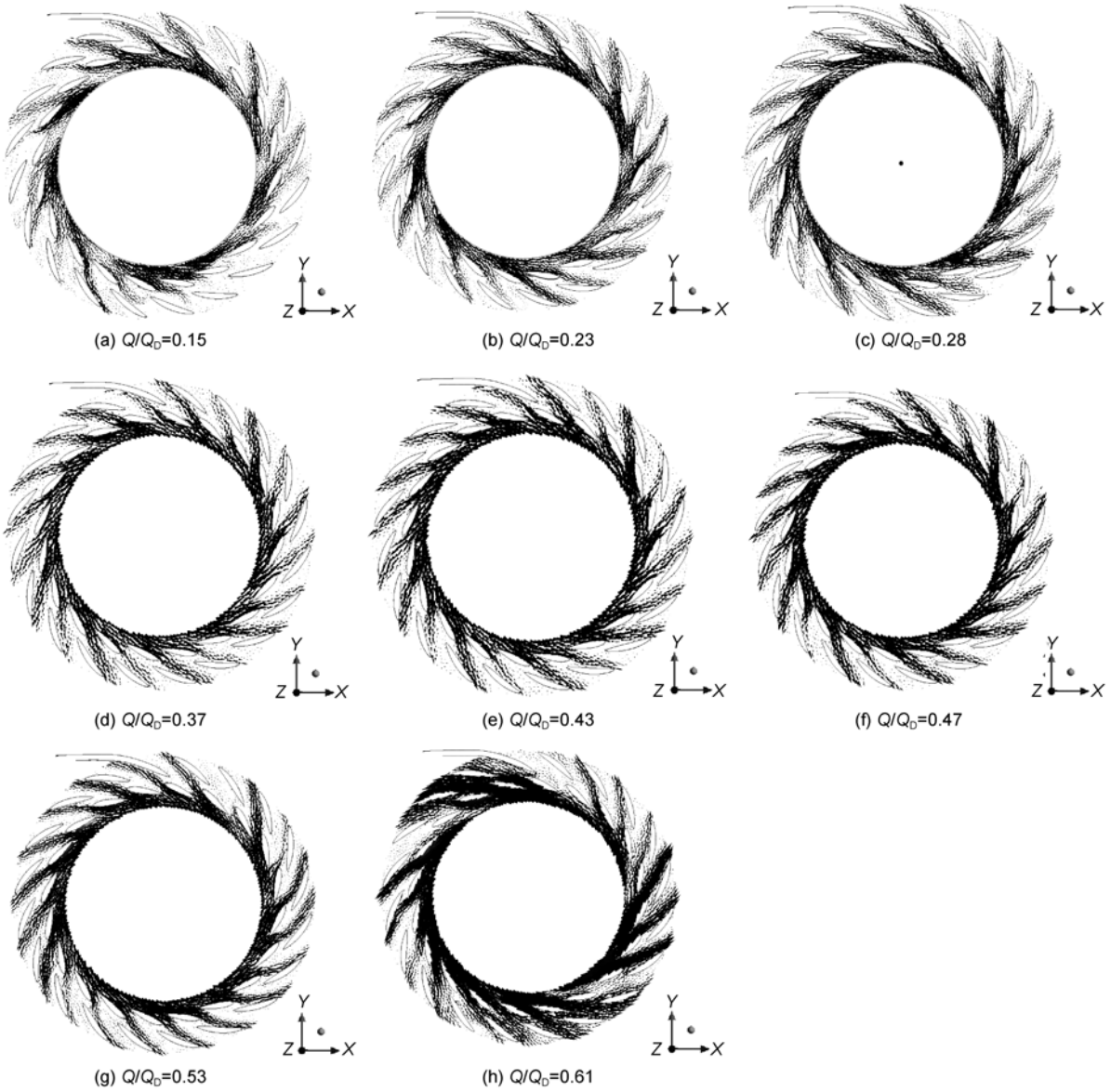

Figure 10 Velocity vectors on P0.1 cross-section for different flow rates.

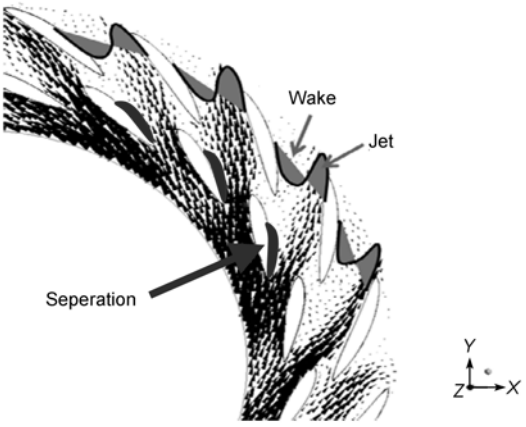

Figure 11 Schematic plot of "jet-wake" flow pattern.

conditions concerned. It is clear that no "jet-wake" feature exists again instead of massive backflow filled in the domain. By comparing P0.9 with P0.5, it can be seen that the tangential velocity becomes prominent in the stay vanes and guide vanes. With the increasing of flow rate, the reversed flow will be weakened gradually. A remarkable transition is found at Q/Q_D=0.61, in which the radial velocity changes to be positive in the circumference direction and chaotic pattern like Figure 8(h) appears. Besides, the flow in spiral casing will undergo a complex process that changes from many vortex structures at Q/Q_D=0.23 to a fluent situation until Q/Q_D=0.53, then is full of secondary flow at Q/Q_D= 0.61.

From the analysis on the velocity vectors in the three cross-sections, it can be concluded that very complex stalled

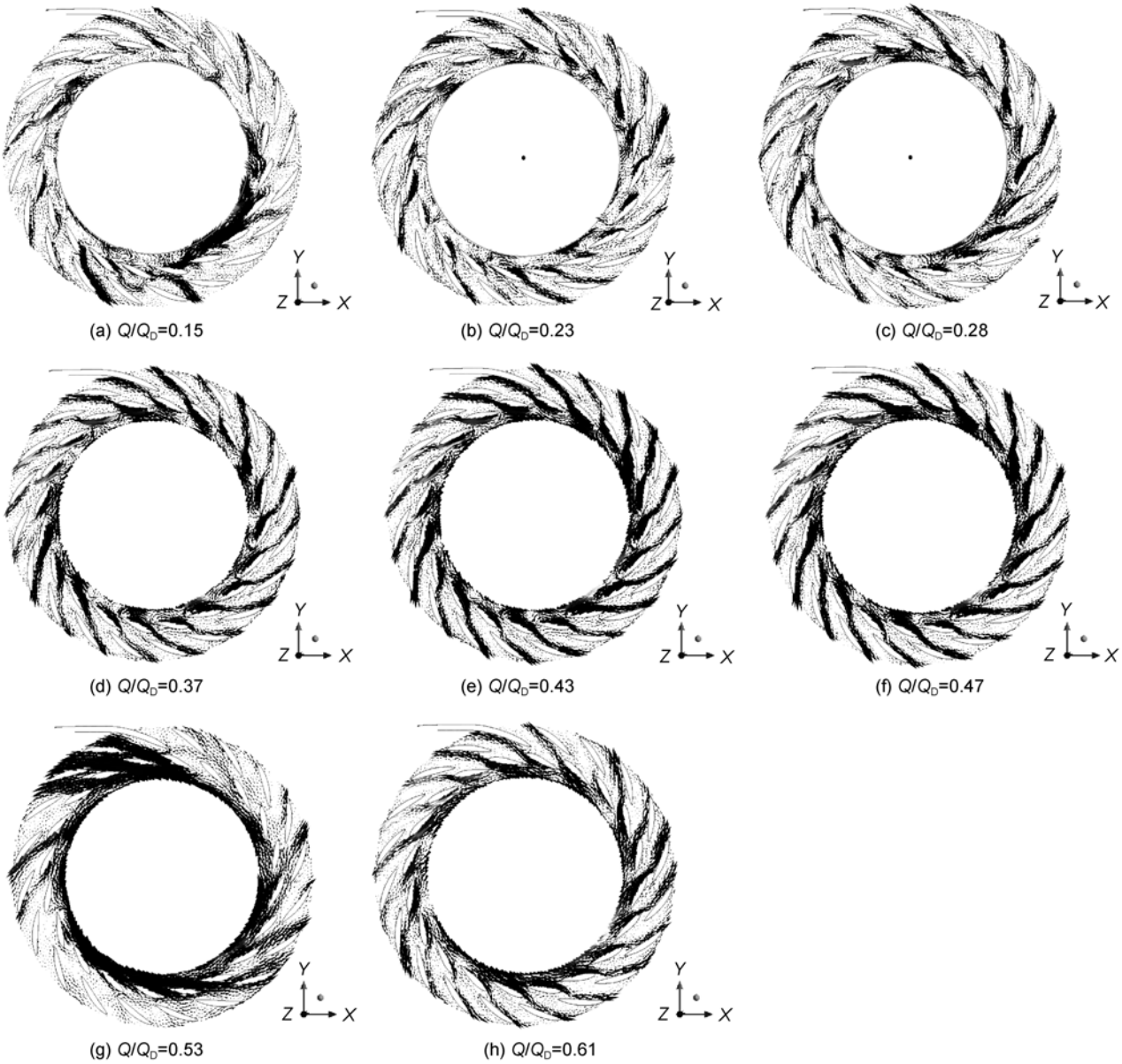

Figure 12 Velocity vectors on P0.5 cross-section for different flow rates.

flow is occupied in the domain of stay vanes and guide vanes. In order to investigate the relationship between the above-mentioned internal flow and the external performance of pump turbine quantificationally, the non-dimen- sional hydraulic loss and the total head without stay vanes and guide vanes are illustrated in Figure 14. It is suggested that the head-flow profile is similar to that of a traditional pump, which will descend monotonously after a positive slope under small flow rates. The positive characteristic is caused by the reverse flow at the inlet [11], while the hydraulic loss of stay vanes and guide vanes changing with flow rate is in a parabolic way. Considering the two profiles, the shape of the head-flow profile of pump turbine is even as seen in Figure 7.

5 Conclusions

Though flow simulation and analysis on the eight operating points under off-design conditions, the following conclusions are drawn.

1) SST k-ω turbulence model is capable of capturing the massively separated flow and can be used to predict the head-flow profile of pump turbine under off-design conditions.

2) Three-dimensional effect is prominent in the flow regime, which can be concluded from comparison between flow features on three axial locations.

3) As the flow rate increases, the “jet-wake” flow feature

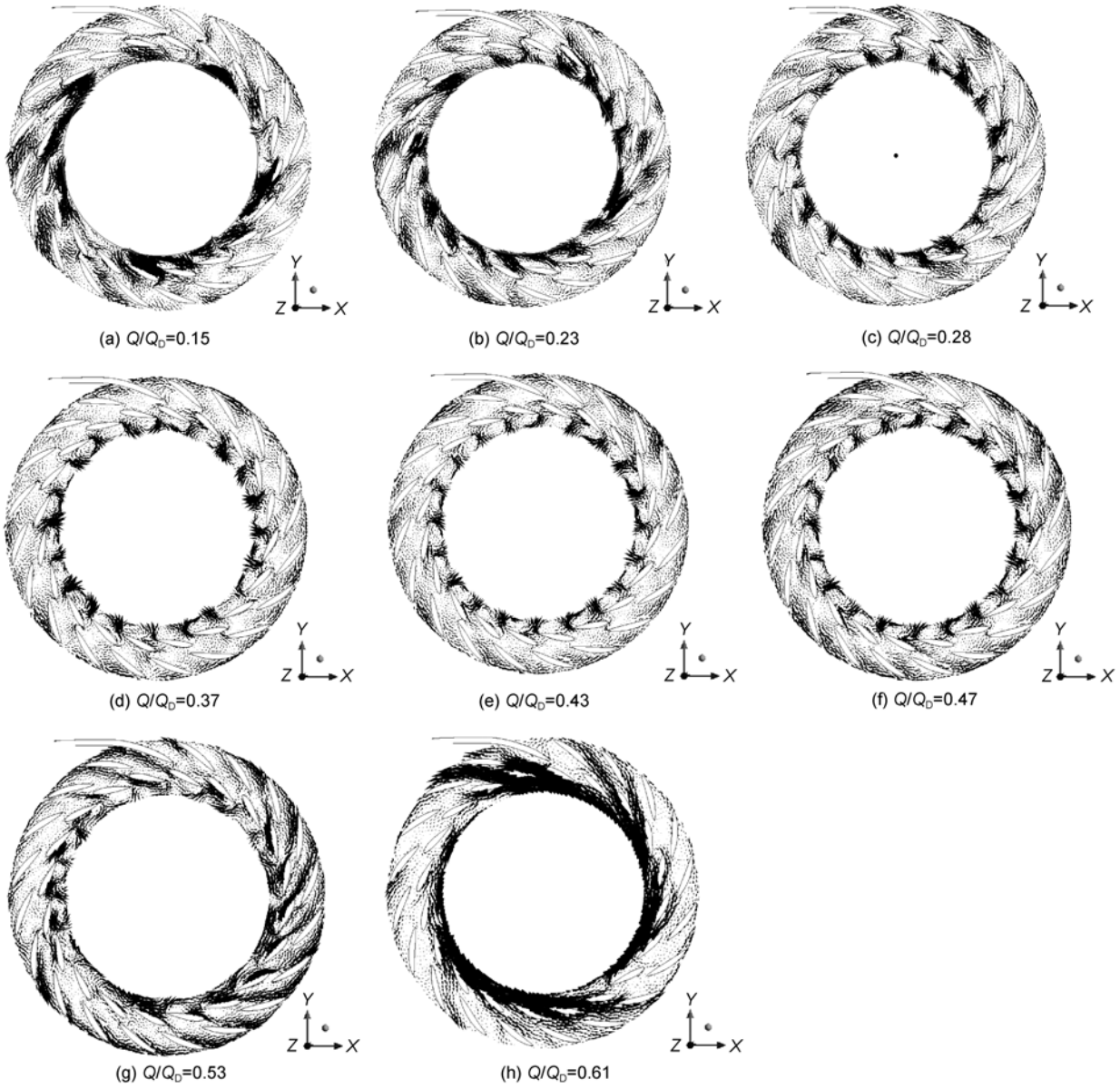

Figure 13 Velocity vectors on P0.9 cross-section under different flow rates.

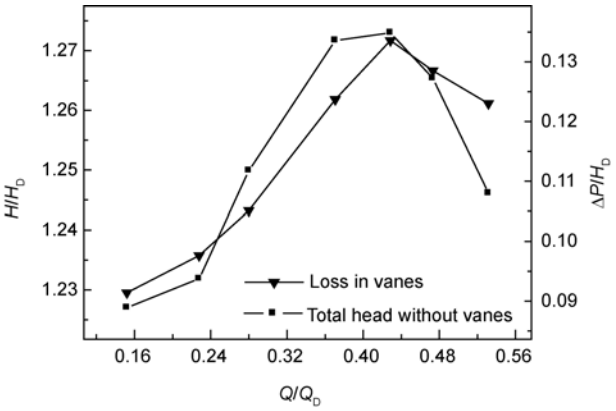

Figure14 Hydraulic losses and vaneless head vs non-dimensional flow rate.

on P0.1 changes little, while great changes are found on P0.5 and P0.9 in that the radial velocity component evolves from negative to positive.

4) The special head-flow profile can be ascribed to the complex flow mechanism of stay vanes and guide vanes, whose parabolic hydraulic characteristic leads to the even shape of the pump turbine's performance.

The work was supported by the National Natural Science of Foundation of China (Grant No. 50979095).

1 Emmons H W, Kronauer R E, Rockett J A, et al. A survey of stall propagation—Experiment and theory. J Basic Eng-Trans ASME, 1959, 81: 409–416

2 Ullum U, Wright J, Dayi O, et al. Prediction of rotating stall within an impeller of a centrifugal pump based on spectral analysis of pressure and velocity data. J Phys-Conf Ser, 2006, 52: 36–45
3 Krause N, Zahringer K, Pap E. Time-resolved particle imaging velocimetry for the investigation of rotating stall in a radial pump. Experiment Fluid, 2005, 39: 192–201
4 Sinha M, Pinarbasi A, Katz J. The flow structure during onset and developed states of rotating stall within a vaned diffuser of a centrifugal pump. J Fluid Eng, 2001, 123: 490–499
5 Guleren K M, Pinarbasi A. Numerical simulation of the stalled flow within a vaned centrifugal pump. J Mech Eng Sci, 2004, 218: 1–11
6 Sun J, Tsukamoto H. Off-design performance prediction for diffuser pumps. Proc Inst Mech Eng, 2001, 215: 191–201
7 Zhang L J, Jin X Y, Chang J S. Flow analysis of the pump turbine runner in the pump mode. Trans Chinese Soc Agr Mach, 2008, 39(4): 69–72
8 Ji X Y, Zhao L Z, Liu S Z. Numerical analysis on Francis pump-turbine of 3D tubulent flow. Large Electr Mach Hydraul Turbine, 2008, 1: 54–58
9 Ran H J, Luo X W, Zhang Y, et al. Numerical simulation of a high-head pump turbine and the runner improvement. In: 11th International Symposium on Advances in Numerical Modeling of Aerodynamics and Hydrodynamics in Turbomachinery. Miami: Fluids Engineering Division, 2006. 1–15
10 Hasmatuchi V, Farhat M, Maruzewski P, et al. Experimental investigation of a pump-turbine at off-design operation conditions. In: Proceedings of the 3rd International Meeting of the Workgroup on Cavitation and Dynamic Problems in Hydraulic Machinery and Systems. Brno: Brno University of Technology, 2009. 339–347
11 Christopher E B. Hydrodynamics of Pumps. Oxford: Oxford University Press, 1994